

Far-red light enhances photochemical efficiency in a wavelength-dependent manner

Shuyang Zhen^{a,†,*}, Mark Haidekker^b and Marc W. van Iersel^a

^aDepartment of Horticulture, University of Georgia, 1111 Miller Plant Science Building, Athens, GA 30602, USA

^bCollege of Engineering, University of Georgia, 597 DW Brooks Drive, Athens, GA 30602, USA

[†]Present address: Department of Plants Soils and Climate, Utah State University, 4820 Old Main Hill, Logan, UT 84322-4820, USA

Correspondence

*Corresponding author,

e-mail: shuyang.zhen@usu.edu

Linear electron transport depends on balanced excitation of photosystem I and II. Far-red light preferentially excites photosystem I (PSI) and can enhance the photosynthetic efficiency when combined with light that over-excites photosystem II (PSII). The efficiency of different wavelengths of far-red light at exciting PSI was quantified by measuring the change in quantum yield of PSII (Φ_{PSII}) of lettuce (*Lactuca sativa*) under red/blue light with narrowband far-red light added (from 678 to 752 nm, obtained using laser diodes). The Φ_{PSII} of lettuce increased with increasing wavelengths of added light from 678 to 703 nm, indicating longer wavelengths within this region are increasingly used more efficiently by PSI than by PSII. Adding 721 nm light resulted in similar Φ_{PSII} as adding 703 nm light, but Φ_{PSII} tended to decrease as wavelength increased from 721 to 731 nm, likely due to decreasing absorbance and low photon energy. Adding 752 nm light did not affect Φ_{PSII} . Leaf chlorophyll fluorescence light response measurements showed lettuce had higher Φ_{PSII} under halogen light (rich in far-red) than under red/blue light (which over-excites PSII). Far-red light is more photosynthetically active than commonly believed, because of its synergistic interaction with light of shorter wavelengths.

Abbreviations – A_n , net photosynthetic rate; Chl, chlorophylls; DLI, daily light integral; F_0 and F_m , minimum and maximum fluorescence yield of dark-adapted leaves, respectively; F_i and F_{m2} steady-state

This is the author manuscript accepted for publication and has undergone full peer review but has not been through the copyediting, typesetting, pagination and proofreading process, which may lead to differences between this version and the Version of Record. Please cite this article as doi: [10.1111/ppl.12834](https://doi.org/10.1111/ppl.12834)

and maximum fluorescence yield of light-adapted leaves, respectively; FWHM, full width at half maximum; LHCII, light harvesting complex II; NPQ, non-photochemical quenching of chlorophyll fluorescence; P_{fr} , far-red light-absorbing phytochrome; PFD, photon flux density; *PPFD*, photosynthetic photon flux density; PPS, phytochrome photostationary state; PQ, plastoquinone; PSI, photosystem I; PSII, photosystem II; ϕ_{PSII} , quantum yield of PSII; SLA, specific leaf area.

Introduction

The efficiency of photosynthesis is wavelength dependent: when measured under monochromatic light, the quantum yield for CO₂ fixation per absorbed photon is higher under red light (about 600-680 nm) than that under blue and green light (Evans 1987, Inada 1976, McCree 1972). Photosynthetic efficiency declines sharply at wavelengths above 685 nm, first described as the 'red drop' by Emerson and Lewis (1943). Absorption by photosynthetic carotenoids (which can transfer excitation energy to chlorophylls (Chl) with an efficiency significantly less than 100%) and non-photosynthetic flavonoids and carotenoids partly account for the lower quantum yield of blue and green light (Hogewoning et al. 2012, Hoover 1937, Terashima et al. 2009). Besides that, a major cause for the wavelength dependency of photosynthetic efficiency is the imbalanced excitation of photosystem I (PSI) and photosystem II (PSII) that carry out the photochemical reactions of photosynthesis (Evans 1987, Hogewoning et al. 2012). Due to differences in pigment composition, antenna size, and density of PSI and PSII, excitation energy distribution between the two photosystems is often imbalanced, especially under narrow spectrum light (Hogewoning et al. 2012, Laisk et al. 2014).

Photochemical efficiency is often measured as the quantum yield of PSII (ϕ_{PSII}) – the fraction of absorbed light that is used for photochemistry to drive electron transport (Genty et al. 1989, Maxwell and Johnson 2000). Under light that over-excites one photosystem relative to the other, the rate of photochemical reactions is limited by the activity of the under-excited photosystem. Photosynthetic responses (e.g., photochemical efficiency and photosynthetic rate) are thus expected to differ under measuring light spectra that excite the photosystems differently (Murakami et al. 2017, Walters 2005). For instance, red/blue light emitting diode (LED) light tends to under-excite PSI (Evans 1987, Hogewoning et al. 2012). Laisk et al. (2014) quantified the electrons transported per photon absorbed by each photosystem of sunflower leaves and confirmed that PSII was over-excited at most of the wavelengths within 400-680 nm, except for at 400-450 nm, and 510, 620 and 680 nm where PSI and PSII had similar quantum yield

for electron transport. Both \dot{J}_{PSII} and net photosynthetic rate (A_n) of lettuce measured under red/blue light emitting diode (LED) increases when far-red light is added to the red/blue measuring light (Zhen and van Iersel 2017). This increase in \dot{J}_{PSII} after adding far-red light differs from the typical decrease in \dot{J}_{PSII} with increasing light intensity (Baker 2008) and is thought to be caused by preferential excitation of PSI by far-red light (Evans 1987, Hogewoning et al. 2012, Laisk et al. 2014, Murakami et al. 2018). This rebalances the excitation between the two photosystems.

The excitation balance between the two photosystems is also affected by acclimation to different light spectra. Plants possess several mechanisms that allow them to dynamically adjust their photosystem composition to optimize photosynthetic efficiency in different light environments. Short-term responses (taking place within minutes) to imbalanced excitation of the two photosystems include the re-allocation of a mobile pool of light harvesting complex II (LHCII) to the under-excited photosystem, a process termed state transitions that directs more energy to the under-excited photosystem (Allen 1992, 2003, Haldrup et al. 2001). Adjustments in photosystem stoichiometry, for example an increase in the PSI/PSII ratio of plants grown under light that over-excites PSII, can take place over days to rebalance excitation of the two photosystems and increase photosynthetic efficiency (Chow et al. 1990, Fujita 1997, Hogewoning et al. 2012). A decrease in the amount of LHCII per PSII core has also been reported in plants grown under blue light (which over-excites PSII), decreasing the amount of excitation energy partitioned to PSII (Hogewoning et al. 2012). Those changes in photosystem composition as a result of acclimation to the light environment may affect how efficiently plants use light of different spectra for photosynthesis, as well as the interactive effects among lights of different wavelengths.

Because most of the shorter wavelength photons within the 400-680 nm range tend to over-excite PSII, while longer wavelength far-red light ($\gg > 680$ nm) tends to strongly over-excite PSI (Evans 1987, Hogewoning et al. 2012, Laisk et al. 2014), the synergistic effect between far-red light and shorter wavelengths is important for enhancement of photosynthesis. The enhancement of photosynthetic rate when combining longer wavelength light ($\gg > 680$ nm) and shorter wavelength light was first shown by Emerson and coworkers over half a century ago (Emerson et al. 1957, Emerson and Rabinowitch 1960). However, it is not clear which wavelengths of far-red light enhance photochemical and photosynthetic efficiency. Previous studies examining the enhancement effect on photosynthesis used far-red light with relatively broad peak. For example, the far-red LED light used in Zhen and van Iersel (2017) had a peak at 735 nm and full width at half maximum (FWHM) of 35 nm. The relative excitation energy distribution

between the two photosystems in the longer wavelength region ($\gg > 680$ nm) so far has only been quantified at a few wavelengths with relatively poor spectral resolution (FWHM >10 nm) (Evans 1987, Hogewoning et al. 2012, Laisk et al. 2014). As a result, there is a lack of knowledge on the wavelength-specific effects of far-red light on photochemistry.

Using laser diodes to obtain narrow-band far-red light (FWHM of 2-3 nm), we aimed to (1) identify the spectral range of far-red light that enhances photochemistry; (2) determine the relative efficiency of far-red light of different wavelengths and intensities at enhancing photochemistry; and (3) determine if acclimation to different light spectra affects the photosynthetic responses measured under different light spectra. Measurements were made on both plants grown under red/blue LED light (which contained no far-red light with $\gg > 700$ nm) and sunlight (rich in far-red light) to test if the photochemical effects of far-red photons are similar in plants acclimated to different light spectra, specifically, with and without a far-red component.

Materials and methods

Plant material and growth conditions

Lettuce (*Lactuca sativa* ‘Green Towers’) was seeded in 1.7-l containers filled with a soilless substrate (Fafard 2P; 60% peat and 40% perlite; Sun Gro Horticulture, Agawam, MA, USA) with controlled-release fertilizer (16N-2.6P-9.9K; Harrell’s 16-6-12, Lakeland, FL) incorporated at a rate of 4.7 g l^{-1} . Seedlings were grown in a growth chamber (E15; Conviron, Winnipeg, MB, Canada) under red/blue LED light (12 h photoperiod at a photosynthetic photon flux density (PPFD) of $202 \pm 36 \mu\text{mol m}^{-2} \text{ s}^{-1}$; 54 W LEDs by PopularGrow, Shenzhen Houyi Lighting, Shenzhen, China) or in a glass-covered greenhouse with no supplemental light. Light intensity inside the greenhouse was measured every 1 s at plant height using quantum sensors (SQ-110; Apogee Instruments, Logan, UT). Plants in the growth chamber were rotated every 2 days throughout the growing period. Four groups of lettuce were seeded every 2 to 3 weeks between 16 December 2016 and 18 February 2017. Measurements of red/blue- and sunlight-grown lettuce were made on plants from the same age groups that were 34 to 43 days old.

The spectral distributions of the different light sources were measured using a spectroradiometer (SS-110; Apogee Instruments, Logan, UT) and normalized to their respective peaks (Fig. 1). The blue (401-500 nm):green (501-600 nm):red (601-700 nm):far-red (701-800 nm) ratio (B:G:R:FR ratio) of the red/blue LED light (peak wavelengths at 634 and 454 nm) was 30:1.8:68.2:0 (each component expressed as % of

total *PPFD*). The B:G:R:FR ratio of sunlight inside the greenhouse (measured around solar noon) was 28.9:35.4:35.7:33.0. Note that sunlight has a large amount of far-red light.

Phytochrome photostationary state (PPS), an indicator of the relative amount of active phytochrome (i.e. far-red light-absorbing form P_{fr}) in plants (Sager et al. 1988), was also estimated using the spectroradiometer (SS-110; Apogee Instruments, Logan, UT). The estimated PPS under the red/blue LED light was 0.88.

Light acclimation and measuring light effects on light responses of Φ_{PSII} and NPQ

Light responses of Φ_{PSII} and non-photochemical quenching of chlorophyll fluorescence (NPQ) of lettuce grown under both sunlight and red/blue light were determined by subjecting plants to increasing *PPFD* (0 to 500 $\mu\text{mol m}^{-2} \text{s}^{-1}$) of red/blue or halogen light (70 W; Sylvania, Wilmington, MA). Halogen light was used as it contains a large amount of far-red light. The B:G:R:FR ratio of the halogen light was 7.0:27.6:65.4:89.2 (Fig. 1). Plants were dark-adapted overnight prior to data collection. Chlorophyll fluorescence measurements were made on recently matured leaves using a pulse-amplitude modulated fluorometer (measuring light peak at 650 nm, mini-PAM; Heinz Walz, Effeltrich, Germany). Minimum and maximum fluorescence yield of dark-adapted leaves (F_0 and F_m , respectively) were determined to calculate the maximum Φ_{PSII} with all the reaction centers being ‘open’ (Q_A , the primary electron acceptor of PSII, maximally oxidized) (Baker 2008). Then, steady-state and maximum fluorescence yield (F_t and F_m2 , respectively) at each *PPFD* level (25 to 500 $\mu\text{mol m}^{-2} \text{s}^{-1}$ of red/blue or halogen light) were determined after plants were given 20 min to stabilize under that light level. Φ_{PSII} of light-adapted leaves was calculated as $\Phi_{PSII} = (F_m2 - F_t) / F_m2$ (Genty et al. 1989), and NPQ was calculated as $\text{NPQ} = (F_m - F_m2) / F_m2$ (Maxwell and Johnson 2000). The fluorescence signal during the saturating light pulse was monitored to assure that the signal saturated during F_m and F_m2 measurements. This entire procedure was replicated three times for both red/blue- and sunlight-grown lettuce. Lettuce used for these measurements received an average DLI of 8.7 $\text{mol m}^{-2} \text{day}^{-1}$ under red/blue light and 8.1 $\text{mol m}^{-2} \text{day}^{-1}$ under sunlight.

Narrow-spectrum far-red light

Laser diodes were used to provide narrow-spectrum far-red light with FWHM of 2-3 nm. Those narrow-spectrum far-red lights were used to determine the responses of Φ_{PSII} to different wavelengths and intensities of far-red light as described in the sections below. The laser diodes are temperature-tunable, i.e.

the peak wavelength shifts toward longer wavelength with increasing temperature. A custom-built temperature controller with a Peltier thermoelectric cooler module (LDM21; Thorlabs, Newton, NJ) was used to control the temperature of the laser within 10 to 60 °C, allowing for a ~10 nm wavelength tuning range for each laser diode. The peak wavelengths at different temperatures were determined using a spectroradiometer (SS-110; Apogee Instruments, Logan, UT). Four non-collimated laser diodes (HL6750MG, HL6738MG, HL7001MG, HL7302MG; Thorlabs, Newton, NJ) were used to provide 18 narrow-bands within the 678-703 nm and 721-731 nm ranges. One additional laser diode (LT031MD; Meredith Instruments, Peoria, AZ) was used to provide a single band centered at 752 nm. Note that the wavelength gaps (704-720 and 732-751 nm) were due to the unavailability of laser diodes emitting at these wavelengths. Lights of wavelengths longer than 752 nm were not included, as our preliminary data indicated that they were ineffective in enhancing photochemistry. For simplicity, we refer to all light wavelengths provided by the laser diodes as far-red light, including those < 700 nm.

Far-red light was projected from above onto the leaf through a diffuser, so that a circular leaf area with a diameter of 4 cm or greater was uniformly lighted. The incident far-red light intensity was measured using a silicon power sensor (S140A; Thorlabs, Newton, NJ) connected to a power meter (PM100; Thorlabs, Newton, NJ). The measured power was converted to photon flux density (PFD) based on the amount of energy contained per mole of photons at different wavelengths and the area of the power sensor sensing area. The light intensity at different temperatures (i.e. different peak wavelengths) was adjusted using a potentiometer, which controlled the current to the laser diode, to obtain an incident PFD of $40 \mu\text{mol m}^{-2} \text{s}^{-1}$. A stable PFD over the entire temperature range was achieved by measuring the power output from the laser diode using the built-in laser monitor diode. The laser drive current was then adjusted using a proportional-controller with an analog circuit to keep the laser output power constant, even when the laser diode efficiency declined at higher temperatures. The position of the power sensor was noted, and subsequent Chl fluorescence measurements were made on leaves placed at the same spot as where the light intensity was measured.

Response of Ψ_{PSII} to different wavelengths of far-red light

The response of Ψ_{PSII} to different wavelengths of far-red light within the 678-752 nm range was quantified to identify the wavelengths of far-red light that enhanced photochemistry. Plants were irradiated with a *PPFD* of $200 \mu\text{mol m}^{-2} \text{s}^{-1}$ red/blue light for about an hour before stabilized Ψ_{PSII} was determined. Then,

far-red light of $40 \mu\text{mol m}^{-2} \text{s}^{-1}$ was added. Ψ_{PSII} was measured shortly (12-15 s) after the addition, and far-red light was then turned off. After 10-15 min, far-red light of a different peak wavelength was added, and Ψ_{PSII} was determined in the same fashion until all the wavelengths of far-red light from each laser diode were added. After that, a different laser diode was calibrated, and Ψ_{PSII} measurements were made in a similar manner as described above. Ψ_{PSII} under $240 \mu\text{mol m}^{-2} \text{s}^{-1}$ red/blue light (i.e. red/blue light intensity increased from $200 \mu\text{mol m}^{-2} \text{s}^{-1}$ by $40 \mu\text{mol m}^{-2} \text{s}^{-1}$) was also determined. This entire procedure was replicated four times for both red/blue- and sunlight-grown lettuce.

Note that a short time period of far-red exposure (12-15 s) was used because it allowed for the effects of far-red light on photochemistry to be quantified without altering non-photochemical processes, e.g., state transitions or xanthophyll cycle activity, that could be affected by far-red light on longer time scales (occur over minutes) (Allen 2003, Haldrup et al. 2001, Zhen and van Iersel 2017).

Sunlight-grown lettuce used for these far-red spectral response measurements received an average DLI of $9.9 \text{ mol m}^{-2} \text{ day}^{-1}$, compared to that of $8.7 \text{ mol m}^{-2} \text{ day}^{-1}$ received by red/blue light-grown lettuce. Leaf light absorbance (Fig. 2) was measured on the same leaves after responses of Ψ_{PSII} to the addition of different wavelengths far-red light were completed.

Response of Ψ_{PSII} to increasing intensity of far-red light

Two wavelengths of far-red light, peaks at 700 or 723 nm (FWHM 2-3 nm), respectively, were used to investigate how Ψ_{PSII} responded to increasing intensity of far-red light. Those two wavelengths were selected due to their contrasting absorbance by the leaf (absorbance at 723 nm was only about half of that at 700 nm). Ten intensities of far-red light ($0-100 \mu\text{mol m}^{-2} \text{s}^{-1}$) were added to red/blue light of $200 \mu\text{mol m}^{-2} \text{s}^{-1}$. Prior to the measurements, plants were allowed to acclimate to red/blue light for at least 40 min to reach a stabilized Ψ_{PSII} . Then, far-red light of a given intensity was added for 12 s before Ψ_{PSII} was determined, and far-red was then switched off. Each determination of Ψ_{PSII} at a different far-red light intensity was about 40 min apart to allow for adjustment of far-red light intensity, and Ψ_{PSII} under red/blue light was re-measured 10 min before each addition of far-red light to adjust for small variations in Ψ_{PSII} , as Chl fluorescence was measured on slightly different parts of the same leaf. This entire procedure was replicated four times for both red/blue- and sunlight-grown lettuce, which received an average DLI of 8.7 and $17.4 \text{ mol m}^{-2} \text{ day}^{-1}$, respectively. Leaf light absorbance at the two wavelengths was measured on the

same leaves after measurements of Ψ_{PSII} with the addition of different intensities of far-red light were completed.

Leaf absorptance, reflectance, and transmission spectra

Leaf absorptance was determined by measuring leaf reflectance and transmission, similar to the method of Nelson and Bugbee (2015). Leaf reflectance was measured using a spectrometer (UniSpec; PP Systems, Amesbury, MA) equipped with a leaf clip. A highly reflective, diffusive white reference standard was used to calibrate the spectrometer. Reflectance of the adaxial side of the leaf was averaged from multiple measurements made on each leaf. The spectrometer measured the spectrum at ~ 3.3 nm intervals, and reflectance was calculated in 1 nm steps by interpolating the measured spectrum, using reverse distance weighting. To determine leaf transmission, a spectroradiometer (SS-110; Apogee Instruments) was placed under a halogen light (same as described above) on a table covered with multiple layers of non-reflective black cloth inside a dark room. Incident light intensity and spectral distribution of the halogen light was determined, and a leaf (adaxial side facing the halogen light) was then placed in between the halogen light and the spectroradiometer to determine the intensity and spectral distribution of the transmitted light (Massa et al. 2015). The Apogee spectroradiometer had a hemispherical (180°) field of view with cosine correction to capture both scattered diffuse and direct light transmitted through the leaves. Leaf absorptance was calculated as $1 - \text{leaf reflectance} - \text{transmission}$. Percent leaf light absorption under different light sources was calculated by multiplying the leaf absorptance spectrum by the spectral distribution of the light sources, and then integrated over a certain wavelength range, e.g., 400-700 nm.

Specific leaf area and pigment analysis

Specific leaf area (SLA, leaf area/dry mass) and pigment composition were determined using lettuce plants that received an average daily light integral (DLI, total *PPFD* integrated over each day) of 8.7 and 9.9 $\text{mol m}^{-2} \text{day}^{-1}$ under red/blue light and sunlight, respectively. Leaf area of three mature leaves per plant (six plants per growth light type, i.e. sunlight or red/blue LED light) was determined. Leaves were then oven-dried and weighed.

For pigment analysis, one leaf disk per leaf (3.14 cm^2) was randomly cut using a cork borer. Leaf margins and main veins were avoided. Leaf tissues were ground with pure methanol and centrifuged. The absorbance of the extract at 666, 653, and 470 nm was measured using a spectrophotometer (Spectronic

20 Genesys; Spectronic Instruments, Rochester, NY). Chlorophyll and total carotenoid concentrations were calculated using the equations from Wellburn (1994). Three leaf discs per plant (subsamples) were sampled, and pigment concentrations were averaged for each plant (three plants per growth light type).

Results

Morphology, pigment composition, and leaf light absorptance

Plants grown under red/blue light had substantially (54%) smaller leaves with lower SLA (i.e. thicker leaves) than plants grown under sunlight (Table 1). Chlorophyll (Chl a + b) and total carotenoid concentrations per unit area were 73 and 38% higher, respectively, in red/blue-grown lettuce than in sunlight-grown plants (Table 1). The Chl a/b ratio was similar in red/blue- and sunlight-grown lettuce (average of 2.74 vs. 2.75; Table 1).

With lower SLA and higher pigment concentration, red/blue-grown lettuce absorbed light more efficiently than sunlight-grown plants at all wavelengths in the range of 400-760 nm, particularly in the green (~550 nm) and far-red (~720 nm) regions, where absorptance is relatively low (Fig. 2) (see Björkman 1981, Terashima et al. 2009). The light absorptance averaged over the 400-700 nm region was 0.93 and 0.90 for lettuce grown under red/blue light and sunlight, respectively. Lettuce grown under red/blue light absorbed 94.6% of red/blue light and 92.6% of the halogen measuring light, while sunlight-grown lettuce absorbed 89.3% of sunlight, 92.2% of the red/blue measuring light, and 88.9% of the halogen measuring light (integrated over the 400-700 nm region).

Light acclimation and measuring light effects on light responses of Ψ_{PSII} and NPQ

The light response of Ψ_{PSII} was affected by the interaction among the light spectrum during growth (sun vs. red/blue light) and the intensity and spectrum of the measuring light (red/blue vs. halogen light) (Fig. 3A, B). Ψ_{PSII} of both red/blue- and sunlight-grown lettuce decreased more slowly with increasing incident *PPFD* of halogen light than with that of red/blue light (Fig. 3A, B). This trend held true after we corrected for the lower leaf absorption of halogen light than that of red/blue light, i.e. on absorbed *PPFD* basis (Fig. S1A,B).

Compared to sunlight-grown lettuce, lettuce grown under red/blue light had higher Ψ_{PSII} under both measuring lights, and the difference was most pronounced when measured under red/blue light at high *PPFD* (Fig. 3A,B). This suggests that the red/blue-grown lettuce may have higher maximum

photosynthetic and/or electron transport capacity, which is consistent with the thicker leaves and higher pigment content.

Non-photochemical quenching (NPQ), an indicator of the amount of absorbed light that is dissipated as heat, of lettuce grown under either sunlight or red/blue LED light was lower under halogen light than that under red/blue measuring light (Fig. 3C,D). This is consistent with the higher Φ_{PSII} under halogen light (Fig. 3A,B). The NPQ of sunlight-grown lettuce increased particularly rapidly in response to increasing intensity of red/blue light, which is consistent with the rapid decrease in Φ_{PSII} observed in sunlight-grown lettuce under increasing red/blue light (Fig. 3B). A lower Φ_{PSII} increases the need for dissipating excess energy as heat.

Response of Φ_{PSII} to different wavelengths of far-red light

Quantum yield of PSII was 0.693 under $200 \mu\text{mol m}^{-2} \text{s}^{-1}$ of red/blue light (Fig. 4). The Φ_{PSII} of both red/blue- and sunlight-grown lettuce decreased upon adding 678 nm light to red/blue light, resulting in a similar Φ_{PSII} as increasing the intensity of red/blue light by the same PFD, i.e. $40 \mu\text{mol m}^{-2} \text{s}^{-1}$ (Fig. 4). Quantum yield of PSII of lettuce grown under both red/blue and sunlight increased linearly as far-red light of longer wavelengths up to 692 nm was added, and then tended to have slower increase as wavelengths further increased to 703 nm (Fig. 4; Fig. S2 for comparison of fluorescence changes upon adding 678 nm and 703 nm light). An increase in Φ_{PSII} , compared to that under a red and blue PFD of $200 \mu\text{mol m}^{-2} \text{s}^{-1}$ without supplemental far-red light, occurred at wavelengths > 686 nm for red/blue-grown lettuce, or > 688 nm for sunlight-grown lettuce (Fig. 4). Adding light at 721 nm resulted in similar Φ_{PSII} as that with 703 nm light added, and also an increase in Φ_{PSII} compared to that under only $200 \mu\text{mol m}^{-2} \text{s}^{-1}$ of red/blue light (Fig. 4). There was a tendency for Φ_{PSII} to decrease as wavelengths increased to 731 nm (Fig. 4), which is likely at least partly due to the drop in absorptance in this region (absorptance decreased from 0.46 to 0.31 for red/blue-grown lettuce as the wavelength increased from 721 to 731 nm, and from 0.37 to 0.26 for sunlight-grown lettuce; Fig. 2A,B).

The magnitude of the increase in Φ_{PSII} in response to the addition of different wavelengths of far-red light that enhanced photochemical efficiency was 32% greater (averaged over the 688-731 nm region) in red/blue-grown lettuce than that in sunlight-grown lettuce (Fig. 4), which could be partly attributable to the 15% higher light absorption in red/blue-grown lettuce within this wavelength range (Fig. 2C).

Due to the unavailability of laser diodes in this wavelength range, there were no measurements made within 732-751 nm. The addition of light at 752 nm did not affect $\dot{\Psi}_{\text{PSII}}$ (Fig. 4).

Response of $\dot{\Psi}_{\text{PSII}}$ to increasing intensity of far-red light

The quantum yield of PSII increased asymptotically with increasing intensity of far-red light (700 or 723 nm; Fig. 5). On an incident light basis and at relatively low far-red PFD ($< 50 \mu\text{mol m}^{-2} \text{s}^{-1}$), 700 nm far-red light was more effective in increasing $\dot{\Psi}_{\text{PSII}}$ than 723 nm light (Fig. 5A,B). This is due to the greater light absorptance at 700 nm than that at 723 nm (absorptance of 0.81 at 700 nm and 0.4 at 723 nm for red/blue-grown lettuce, and of 0.74 at 700 nm and 0.32 at 723 nm for sunlight-grown lettuce). On an absorbed light basis, both 700 nm and 723 nm light resulted in similar increases in $\dot{\Psi}_{\text{PSII}}$ for lettuce grown under each growth light (Fig. 5C,D).

Of the $200 \mu\text{mol m}^{-2} \text{s}^{-1}$ incident red/blue light, a comparable amount of light was absorbed by red/blue- and sunlight-grown lettuce (189 vs 184 $\mu\text{mol m}^{-2} \text{s}^{-1}$ absorbed). Red/blue-grown lettuce, however, required a larger amount of absorbed far-red light (e.g. about 32 $\mu\text{mol m}^{-2} \text{s}^{-1}$ of absorbed 700 nm light vs. 11 $\mu\text{mol m}^{-2} \text{s}^{-1}$ needed by sunlight-grown lettuce) before $\dot{\Psi}_{\text{PSII}}$ reached a maximum; the maximum increase in $\dot{\Psi}_{\text{PSII}}$ was also larger in red/blue-grown lettuce compared to that in sunlight-grown lettuce (Fig. 5C,D).

Discussion

The morphology of lettuce grown under red/blue light or sunlight differed substantially, with smaller leaves and lower SLA in plants grown under red/blue light. A lower SLA, or thickening of leaves, can result from acclimation to high light and/or a high fraction of blue light (Björkman 1981, Evans and Poorter 2001, Givnish 1988, Hogewoning et al. 2010). However, lettuce grown under red/blue light received less light than those grown under sunlight (average DLI of 8.7 vs. 9.9 $\text{mol m}^{-2} \text{day}^{-1}$) and similar percentage of blue light (30.0 vs 28.9% of total *PPFD* under red/blue light and sunlight, respectively). Another cause for a decrease in SLA is acclimation to high red:far-red light environment (McLaren and Smith 1978, Shibuya et al. 2016). Sunlight contained a substantial amount of far-red light, while the red/blue LED light had no far-red (Fig. 1). The lack of far-red light (thereby a high red/far-red ratio) may have contributed to the lower SLA observed in lettuce grown under red/blue light. However, there were other differences in the light environment between the growth chamber and greenhouse, such as a lack of green and yellow light in the growth chamber, which may have contributed to morphological differences.

Both red/blue- and sunlight-grown lettuce had higher leaf light absorption than the commonly assumed 84% absorption of incident *PPFD* by green leaves, which was derived from the average absorption of 37 C_3 species under a filtered quartz-halogen light source that was rich in red, yellow, and green light (501-700 nm; peak wavelength at ~680nm), but low in blue light (401-500 nm) (Björkman and Demmig 1987). Leaf light absorptance averaged over the 400-700 nm range under a particular light source is dependent on the spectral distribution of that light. For example, light absorption of a typical green leaf is higher under a light source that is rich in blue and red photons (e.g. red/blue LEDs) than one that contains more green photons (e.g. halogen light or sunlight). Other factors that determine light absorption, including leaf structure, pigment composition and concentration, often vary among species and are affected by growth conditions. For instance, the lettuce used in our study was fertilized, while the species used by Björkman and Demmig (1987) were mostly from native habitats and local gardens and likely not fertilized, which may result in lower Chl concentrations. In addition, Björkman and Demmig (1987) determined the leaf absorption spectrum at 25 nm intervals, which could compromise the accuracy of the measurements. Therefore, the commonly assumed 84% absorption of incident *PPFD* may not be an accurate estimate of light absorption by a specific leaf under a certain light source.

Note that an integrating sphere is often used in determination of leaf light reflectance and transmission. We compared leaf absorptance measurements made using our method with those obtained using an integrating sphere (DeLucia et al. 1996, Hogewoning et al. 2010, Olascoaga et al. 2016) and found that the characteristics and the values of the absorptance curves by the two methods matched well within the 400-700 nm region. The absorptance in the near infrared region (701-760 nm), however, tended to be higher when measured by our method than that by an integrating sphere. This could be due to the different species and growth conditions used in the studies (Nelson and Bugbee, 2015).

The photochemical effect of different wavelengths of far-red light was determined under equal incident light intensity (Fig. 4), and was thus not influenced by the leaf light absorptance measurements. The response of Ψ_{PSII} to increasing intensity of far-red light on absorbed light basis (Fig. 5 C,D), however, could be affected by inaccuracy in light absorptance measurements. We re-analyzed the data presented in Fig. 5 (C and D) assuming that there was a 10% error in our light absorptance data. The response of Ψ_{PSII} to adding 700 and 723 nm lights were minimally affected, i.e. similar increases in Ψ_{PSII} when adding 700 nm and 723 nm light on an absorbed light basis (data not shown). We do, however, advise caution when considering the absorptance values in the far-red region.

One possible cause for the difference in the responses of Φ_{PSII} to the measuring light spectrum (i.e. higher Φ_{PSII} under halogen- than under red/blue-measuring light on both incident and absorbed *PPFD* basis) is that the excitation energy distribution between PSI and PSII differs under red/blue and halogen light. Red and blue light tends to overexcites PSII relative to PSI (Evans 1987, Hogewoning et al. 2012, Laisk et al. 2014). When PSII is over-excited, the plastoquinone (PQ) pool, an intermediate electron transporter between PSII and PSI, gradually becomes reduced due to faster influx of electrons from PSII into the PQ pool than they can leave it (Allen 2003). Consequently, a greater fraction of the PSII reaction centers become closed, leading to a decrease in Φ_{PSII} . Halogen light, in contrast, contains a large amount of far-red light (Fig. 1) that preferentially excites PSI, resulting in faster re-oxidation of the PQ pool and re-opening of the PSII reaction center (Baker 2008, Bonaventura and Myers 1969, Zhen and van Iersel 2017). Recent studies also showed that the addition of far-red light to fluctuating light helped to alleviate PSI photoinhibition and optimize photosynthesis by keeping P700 in a more oxidized state (Kono et al. 2017, Yamori 2016).

State transition may also play a role in balancing the excitation distribution between PSI and PSII (Allen 2003). As red/blue LED light over-excites PSII, the mobile pool of LHCII is expected to migrate to PSI (State 2). This directs a larger fraction of the excitation energy to PSI and helps to maintain a relatively high PSII quantum yield. Halogen light had a large fraction of far-red light (89.2% of *PPFD*) that preferentially excited PSI. Therefore, lettuce under halogen light was likely to have had the LHCII attached to PSI (State 1). The occurrence of state transition would thus reduce the difference in Φ_{PSII} under RB light and halogen light. As seen in Fig. 3, the difference in Φ_{PSII} between the two measuring lights was evident, indicating that state transition, if occurred, played a limited role in re-balancing excitation among the two photosystems.

In addition to the much larger amount of far-red, halogen light contains a substantially smaller fraction of blue photons and a much larger fraction of green photons than red/blue light (Fig. 1), which may lead to more even vertical light distribution within a leaf under halogen light (Terashima et al. 2009). Under red/blue light, however, a higher proportion of light is likely absorbed by the upper palisade cells near the adaxial surface of the leaf (Brodersen and Vogelmann, 2010). As our fluorometer (Mini-PAM; Heinz Walz) uses a red measuring light (650 nm) that is mainly absorbed by the upper illuminated surface of the leaf, fluorescence emitted from chloroplasts near the illuminated leaf surface is preferentially detected (Terashima et al. 2009). Because Φ_{PSII} typically decreases with increasing absorbed *PPFD* (Baker 2008;

also see Fig. S1), it is possible that the higher absorption of red and blue photons by the upper palisade parenchyma cells contributed to the lower Φ_{PSII} observed under red/blue light than under halogen light.

Quantum yield of CO_2 assimilation correlates with Φ_{PSII} in the absence of photorespiration (Baker 2008, Genty et al. 1989). Therefore, an increase in Φ_{PSII} would likely translate into increase in A_n . Zhen and van Iersel (2017) showed that a 7.5% increase in Φ_{PSII} upon adding far-red light ($90 \mu\text{mol m}^{-2} \text{s}^{-1}$ within 700-770 nm) to a red/blue measuring light ($200 \mu\text{mol m}^{-2} \text{s}^{-1}$) resulted in a 18% increase in A_n of lettuce. Note that the added far-red LED light contained a small amount fraction of photons < 700 nm and caused a 4% increase in *PPFD*, which also contributed to the observed increase in A_n . Whole-plant gas exchange measurements of lettuce under red/blue light and red/blue plus far-red light indicated that adding far-red photons (10-30% of *PPFD*) caused similar increase in whole canopy photosynthetic rate as adding the same amount of red/blue photons (Zhen and Bugbee, unpublished results). In addition to its direct photosynthetic effect, far-red light has also been shown to induce leaf expansion mediated by phytochromes, thus promoting canopy light interception and indirectly increasing plant growth during long-term cultivation (Park and Runkle 2017).

Similar to the observed differences in the light responses of Φ_{PSII} and NPQ, the light response of A_n has also been shown to depend on the interaction of growth light acclimation and the spectrum of the measuring light (Murakami et al. 2017). This is likely associated with differences in photochemical efficiency as indicated by our Φ_{PSII} data. Therefore, evaluation of A_n among plants acclimated to different light spectra should account for the effect of the spectrum of the measuring light, as a mismatch between growth and measuring light could result in estimations of A_n that do not reflect the rate of photosynthesis under the light that plants were grown (Murakami et al. 2017, Walters 2005). This has important implications for leaf gas exchange systems, which commonly use a combination of red and blue LED light as measuring light. As red and blue light under-excites PSI (Hogewoning et al. 2012, Laisk et al. 2014), this likely leads to an underestimation of the photosynthetic rate under sunlight, which contains a substantial amount of far-red light.

To identify the spectral range of far-red light that enhances photochemistry, we quantified the response of Φ_{PSII} to the addition of narrow-band far-red light. The Φ_{PSII} of both red/blue- and sunlight-grown lettuce decreased upon adding 678 nm light to red/blue light to the same extent as increasing the intensity of red/blue light by the same PFD, i.e. $40 \mu\text{mol m}^{-2} \text{s}^{-1}$ (Fig. 4). This suggests that the excitation energy of light at 678 nm was distributed similarly between the two photosystems as that of red/blue light. Φ_{PSII} of

lettuce grown under both red/blue and sunlight increased linearly as far-red light with longer wavelengths up to 692 nm was added, and then tended to have slower increase as wavelength further increased to 703 nm (Fig. 4), indicating that the relative excitation energy distribution gradually shifted toward PSI as wavelengths increased from 678 nm to 703 nm. This shift in excitation energy distribution towards PSI can alleviate over-excitation of PSII relative to PSI, thus resulting in smaller decrease in $\dot{\Phi}_{\text{PSII}}$ compared to that when adding light that more strongly over-excites PSII, e.g., 678 nm. An increase in $\dot{\Phi}_{\text{PSII}}$ (thus enhancement of photochemistry) occurs when the added light preferentially excites PSI (Zhen and van Iersel 2017). Such an increase in $\dot{\Phi}_{\text{PSII}}$, compared to that under a red/blue *PPFD* of $200 \mu\text{mol m}^{-2} \text{s}^{-1}$ without supplemental far-red light, occurred at wavelengths $> 686 \text{ nm}$ for red/blue-grown lettuce, or $> 688 \text{ nm}$ for sunlight-grown lettuce (Fig. 4), indicating that these wavelengths of light over-excited PSI (Baker 2008, Bonaventura and Myers 1969, Zhen and van Iersel 2017). The tendency for greater increases in $\dot{\Phi}_{\text{PSII}}$ at longer wavelengths (up to 703 nm) suggests that light of longer wavelengths increasingly over-excited PSI more than PSII, presumably due to the increasingly lower absorption by PSII than by PSI at longer wavelengths (Hogewoning et al. 2012). It is important to note that leaf light absorbance decreased with increasing wavelength, from 0.94 at 686 nm to 0.79 at 703 nm for red/blue-grown lettuce and from 0.92 at 688 nm to 0.68 at 703 nm for sunlight-grown lettuce (Fig. 2A), meaning that on absorbed light basis, light of longer wavelengths resulted in greater enhancement of $\dot{\Phi}_{\text{PSII}}$. This is consistent with our hypothesis that longer wavelength light increasingly over-excited PSI compared to PSII. However, even PSII has been shown to have some activity when exposed to wavelengths of up to 780 nm (Pettai et al 2005).

Our data suggest that 721 nm light still effectively and preferentially excited PSI (Fig. 4). Hogewoning et al. (2012) showed that the absorbance of purified PSII was close to zero at wavelengths $> 700 \text{ nm}$, whereas purified PSI still had some absorbance at wavelengths $> 721 \text{ nm}$. The addition of light at 752 nm did not affect $\dot{\Phi}_{\text{PSII}}$ (Fig. 4). It is possible that photons with wavelength of 752 nm do not contain enough energy to drive the photochemical reactions in PSI or is not absorbed by photosynthetic pigments. Our data suggest that the upper wavelength limit of light that preferentially drives PSI (and thus enhances photochemistry) falls within the 731-752 nm range.

The asymptotical increase in $\dot{\Phi}_{\text{PSII}}$ with increasing intensity of far-red light (Fig. 5) indicated that the excitation balance between the two photosystems was gradually restored when more far-red light was added to red/blue light. Far-red light can increase $\dot{\Phi}_{\text{PSII}}$ when the rate of photochemical reactions is limited

by the activity of PSI, but increasing far-red light results in no further increases in ψ_{PSII} once PSI is no longer under-excited compared to PSII.

Red/blue-grown lettuce was more responsive to far-red light, with higher maximum increase in ψ_{PSII} caused by far-red addition compared to sunlight-grown lettuce (Fig. 5C, D). One possible explanation for this is that lettuce grown under red/blue light may have more PSI to correct for under-excitation of PSI (Chow et al. 1990, Fujita 1997, Hogewoning et al. 2012), thus requiring a greater amount of far-red light to saturate PSI. In addition, lettuce grown under red/blue light also had thicker leaves with higher pigment concentration and were likely able to absorb and use more far-red light per unit leaf area.

Because of the important effects of far-red light on ψ_{PSII} , as well as on leaf CO_2 exchange (Zhen and van Iersel 2017), we recommend that leaf gas exchange systems include far-red light in the measuring light to better mimic photosynthetic responses under sunlight. Based on our findings, far-red light has photosynthetic activity at 731, but not 752 nm. Since the PFD of far-red light from 701 to 740 nm in sunlight is ~12.5% of *PPFD*, we suggest that photosynthetic measuring light should include far-red at a PFD of 10-15% of *PPFD*. Based on the spectral response of ψ_{PSII} to far-red light (Fig. 4), we suggest that LEDs with a peak wavelength around 710-735 nm be used.

Conclusions

Acclimation to different growth light spectra (red/blue light or sunlight) and the spectrum of the measuring light (red/blue or halogen light) interactively affect the light response of ψ_{PSII} , likely via affecting the excitation balance between PSI and PSII. Far-red light is important in such interaction due to its role in exciting PSI, and should be included in the measuring light of leaf gas exchange systems to improve the accuracy of photosynthetic measurements. Far-red light of wavelengths within the 678-752 nm range differ in their efficiency at exciting PSI and enhancing photochemistry under light that over-excites PSII. Longer wavelengths within 678-703 nm are increasingly used more efficiently by PSI than by PSII, as indicated by the increasing ψ_{PSII} when light of longer wavelengths was added. Light of wavelengths within 686 (or 688) to 731 nm enhanced ψ_{PSII} of lettuce grown under red/blue light (or sunlight) when added to red/blue measuring light, but the efficiency of these wavelengths of light at enhancing ψ_{PSII} tended to decrease as wavelength increased from 721 to 731 nm, probably due to the lower leaf light absorbance at longer wavelengths. Light of 752 nm did not affect ψ_{PSII} . Our data indicate

that the upper wavelength limit of light that enhances photochemistry falls in between the 731-752 nm range.

Acknowledgements – This work was supported by Georgia Research Alliance and USDA National Institute of Food and Agriculture [Hatch project 1011550]. We thank Sue Dove and Michael Martin for technical support.

References

- Allen JF (1992) Protein phosphorylation in regulation of photosynthesis. *Biochim Biophys Acta* 1098: 275-335
- Allen JF (2003) State transitions – a question of balance. *Science* 299: 1530-1532
- Baker NR (2008) Chlorophyll fluorescence, a probe of photosynthesis in vivo. *Annu Rev Plant Biol* 59: 89-113
- Björkman O (1981) Responses to different quantum flux densities. In: Lange OL, Nobel PS, Osmond CB, Ziegler H (eds) *Physiological plant ecology I. Encyclopedia of plant physiology*, vol 12A. Springer-Verlag, Berlin, pp 57-107
- Björkman O, Demmig B (1987) Photon yield of O₂ evolution and chlorophyll fluorescence characteristics at 77k among vascular plants of diverse origins. *Planta* 170: 489–504
- Bonaventura C, Myers J (1969) Fluorescence and oxygen evolution from *Chlorella pyrenoidosa*. *Biochim Biophys Acta* 189: 366-383
- Brodersen CR, Vogelmann TC (2010) Do changes in light direction affect absorption profiles in leaves? *Functional Plant Biol* 37: 403-412
- Chow WS, Melis A, Anderson JM (1990) Adjustments of photosystem stoichiometry in chloroplasts improve the quantum efficiency of photosynthesis. *Proc Natl Acad Sci USA* 87: 7502-7506
- DeLucia EH, Nelson K, Vogelmann TC, Smith WK (1996) Contribution of intercellular reflectance to photosynthesis in shade leaves. *Plant Cell Environ* 19: 159-170
- Emerson R, Chalmers R, Cederstrand C (1957) Some factors influencing the long-wave limit of photosynthesis. *Proc Natl Acad Sci USA* 43: 133-143

- Emerson R, Lewis CM (1943) The dependence of the quantum yield of chlorella photosynthesis on wave length of light. *Am J Bot* 30: 165-178
- Emerson R, Rabinowitch E (1960) Red drop and role of auxiliary pigments in photosynthesis. *Plant Physiol* 35: 477-485
- Evans JR (1987) The dependence of quantum yield on wavelength and growth irradiance. *Aust J Plant Physiol* 14: 69-79
- Evans JR, Poorter H (2001) Photosynthetic acclimation of plants to growth irradiance: the relative importance of specific leaf area and nitrogen partitioning in maximizing carbon gain. *Plant Cell Environ* 24: 755-767
- Fujita Y (1997) A study on the dynamic features of photosystem stoichiometry: Accomplishments and problems for future studies. *Photosyn Res* 53: 83-93
- Genty B, Briantais JM, Baker NR (1989) The relationship between the quantum yield of photosynthetic electron transport and quenching of chlorophyll fluorescence. *Biochim Biophys Acta* 990: 87-92
- Givnish TJ (1988) Adaptation to sun and shade, a whole-plant perspective. *Aust J Plant Physiol* 15: 63-92
- Haldrup A, Jensen PE, Lunde C, Scheller HV (2001) Balance of power: a view of the mechanism of photosynthesis state transitions. *Trends Plant Sci* 6: 301-305
- Hogewoning SW, Douwstra P, Trouwborst G, van Ieperen W, Harbinson J (2010) An artificial solar spectrum substantially alters plant development compared with usual climate room irradiance spectra. *J Exp Bot* 61: 1267-1276
- Hogewoning SW, Trouwborst G, Maljaars H, Poorter H, van Ieperen W, Harbinson J (2010) Blue light dose-responses of leaf photosynthesis, morphology, and chemical composition of *Cucumis Sativus* grown under different combinations of red and blue light. *J Exp Bot* 61: 3107-3117
- Hogewoning SW, Wientjes E, Douwstra P, Trouwborst G, van Ieperen W, Groce R, Harbinson J (2012) Photosynthetic quantum yield dynamics: From photosystems to leaves. *Plant Cell* 24: 1921-1935
- Hoover WH (1937) The dependence of carbon dioxide assimilation in a higher plant on wavelength of radiation. *Smithsonian Institution Misc Collections* 95: 1-13
- Inada K (1976) Action spectra for photosynthesis in higher plants. *Plant Cell Physiol* 17: 355-365
- Kono M, Yamori W, Suzuki Y, Terashima I (2017) Photoprotection of PSI by far-red light against the fluctuating light-induced photoinhibition in *Arabidopsis thaliana* and field-grown plants. *Plant Cell Physiol* 58: 35-45

- Laisk A, Oja V, Eichelmann H, Dall'Osto L (2014) Action spectra of photosystems II and I and quantum yield of photosynthesis in leaves in State 1. *Biochim Biophys Acta* 1837: 315-325
- Massa G, Graham T, Haire T, Flemming C II, Newsham G, Wheeler R (2015) Light-emitting diode light transmission through leaf tissue of seven different crops. *Hort Science* 50: 501-506
- Maxwell K, Johnson GN (2000) Chlorophyll fluorescence – a practical guide. *J Exp Bot* 51: 659-668
- McCree KJ (1972) The action spectrum, absorptance and quantum yield of photosynthesis in crop plants. *Agric Meteorol* 9: 191-216
- Mclaren JS, Smith H (1978) Phytochrome control of the growth and development of *Rumex obtusifolius* under simulated canopy light environments. *Plant Cell Environ* 1: 61-67
- Murakami K, Matsuda R, Fujiwara K (2017) A basis for selecting light spectral distribution for evaluating leaf photosynthetic rates of plants grown under different light spectral distributions. *Environ Control Biol* 55: 1-6
- Murakami K, Matsuda R, Fujiwara K (2018) Quantification of excitation energy distribution between photosystems based on a mechanistic model of photosynthetic electron transport. *Plant Cell Environ* 41: 148-159
- Nelson JA, Bugbee B (2015) Analysis of environmental effects on leaf temperature under sunlight, high pressure sodium and light emitting diodes. *PLoS ONE* 10: e0138930
- Olascoaga B, Mac Arthur A, Atherton J, Porcar-Castell A (2016) A comparison of methods to estimate photosynthetic light absorption in leaves with contrasting morphology. *Tree Physiol* 36: 368-379
- Park Y, Runkle ES (2017) Far-red radiation promotes growth of seedlings by increasing leaf expansion and whole-plant net assimilation. *Environ Exp Bot* 136: 41-49
- Pettai H, Oja V, Freiberg A, Laisk A (2005) Photosynthetic activity of far-red light in green plants. *Biochim Biophys Acta - Bioenergetics* 1708: 311-321
- Sager JC, Smith WO, Edwards JL, Cyr KL (1988) Photosynthetic efficiency and phytochrome photoequilibria determination using spectral data. *Trans ASAE* 31: 1882-1889
- Shibuya T, Endo R, Kitaya Y, Hayashi S (2016) Growth analysis and photosynthesis measurements of cucumber seedlings grown under light with different red to far-red ratios. *HortScience* 51: 843-846
- Terashima I, Fujita T, Inoue T, Chow WS, Oguchi R (2009) Green light drives leaf photosynthesis more efficiently than red light in strong white light: revisiting the enigmatic question of why leaves are green. *Plant Cell Physiol* 50: 684-697

- Walters RG (2005) Towards an understanding of photosynthetic acclimation. *J Exp Bot* 56: 435-447
- Wellburn AR (1994) The spectral determination of chlorophylls a and b, as well as total carotenoids, using various solvents with spectrophotometers of different resolution. *J Plant Physiol* 144: 307-313
- Yamori W (2016) Photosynthetic response to fluctuating environments and photoprotective strategies under abiotic stress. *J Plant Res* 129: 379-395
- Zhen S, van Iersel MW (2017) Far-red light is needed for efficient photochemistry and photosynthesis. *J Plant Physiol* 209: 115-122

Supporting information

Additional supporting information may be found in the online version of this article

Fig. S1. Light responses of Φ_{PSII} and NPQ to increasing *PPFD* on an absorbed light basis.

Fig. S2. Comparison of fluorescence changes upon adding 678 nm and 703 nm light to a background red/blue light.

Figure legends

Fig. 1. Normalized spectral distribution of sunlight, red/blue light-emitting diodes (LED) light, and halogen light.

Fig. 2. Absorbance, transmission, and reflectance spectra of red/blue-grown lettuce leaves (A) and sunlight-grown lettuce leaves (B). Measurements were made on the same leaves that were used to quantify the responses of Φ_{PSII} to the addition of different wavelengths far-red light. Sunlight-grown lettuce received an average DLI of $9.9 \text{ mol m}^{-2} \text{ day}^{-1}$ while red/blue-grown lettuce received an average DLI of $8.7 \text{ mol m}^{-2} \text{ day}^{-1}$. Absorbance ratio is calculated as absorbance of red/blue-grown lettuce to that of sunlight-grown lettuce (C).

Fig. 3. Quantum yield of photosystem II (Φ_{PSII}) (A, B) and non-photochemical quenching (NPQ) (C, D) of lettuce grown under red/blue light (A, C) or sunlight (B, D) in response to increasing incident photosynthetic photon flux density (*PPFD*) of red/blue light or halogen light. Error bars indicate \pm SE. ($n = 3$).

Fig. 4. Quantum yield of photosystem II (Φ_{PSII}) upon adding different wavelengths of far-red light (FWHM 2-3 nm) to red/blue light for lettuce grown under red/blue light (A) or sunlight (B). Each far-red wavelength was added at an incident photon flux density of $40 \mu\text{mol m}^{-2} \text{ s}^{-1}$. Long-dashed line (top) indicates the initial Φ_{PSII} under red/blue light of $200 \mu\text{mol m}^{-2} \text{ s}^{-1}$, and the short-dashed line (bottom) indicates Φ_{PSII} under red/blue light of $240 \mu\text{mol m}^{-2} \text{ s}^{-1}$. Error bars indicate \pm SE. ($n = 4$).

Fig. 5. Quantum yield of photosystem II (ϕ_{PSII}) as a function of the incident photon flux density (PFD) (A, B) and absorbed PFD (C, D) of far-red light with a peak wavelength of 700 or 723 nm, respectively. Lettuce grown under red/blue light (A, C) or sunlight (B, D) and measured under $200 \mu\text{mol m}^{-2} \text{s}^{-1}$ of red/blue light with the addition of different intensities of far-red light. Error bars indicate \pm SE. ($n = 4$).

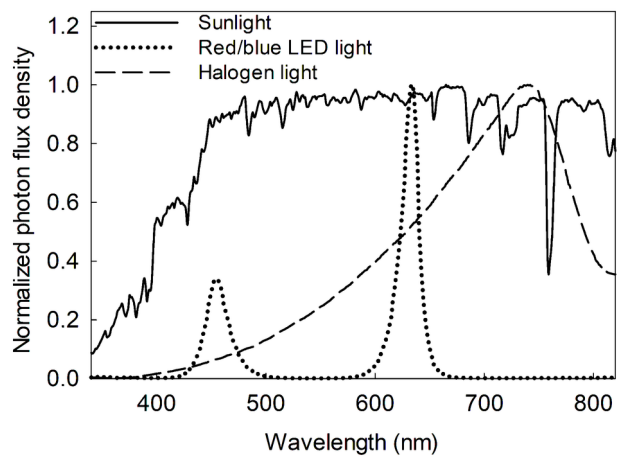


Fig. 1.TIF

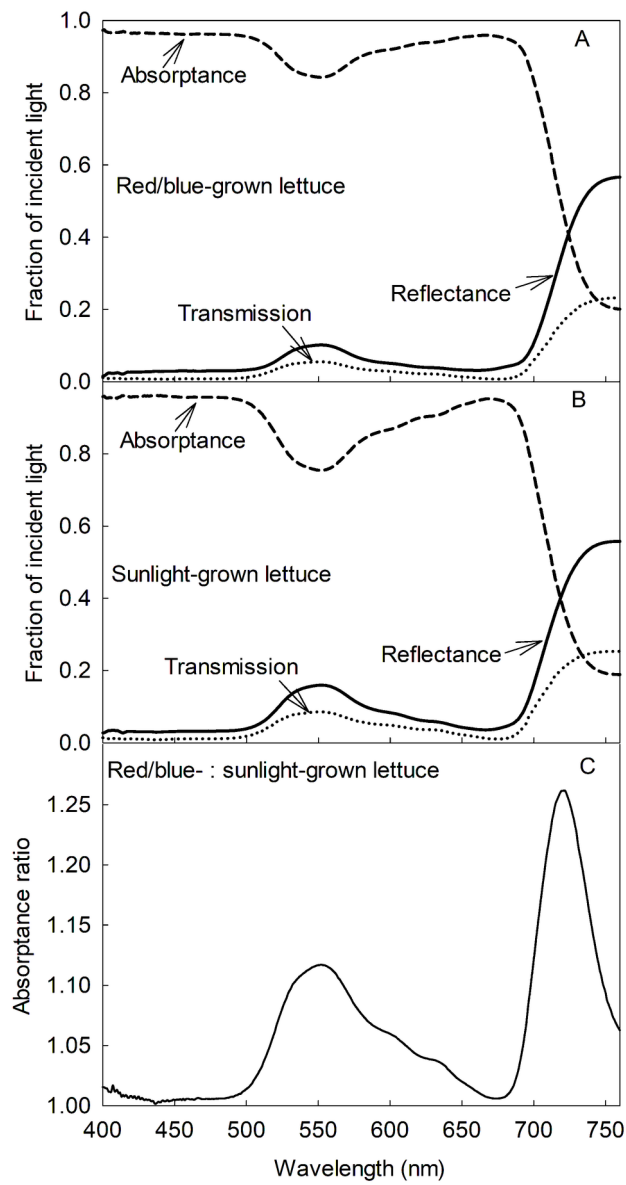


Fig. 2.TIF

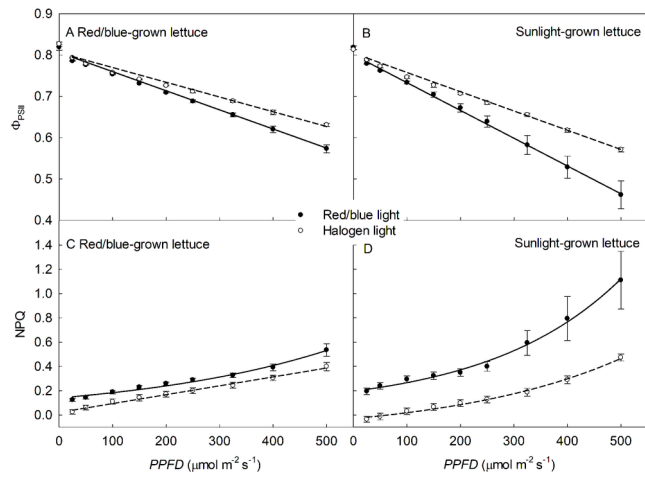


Fig. 3.TIF

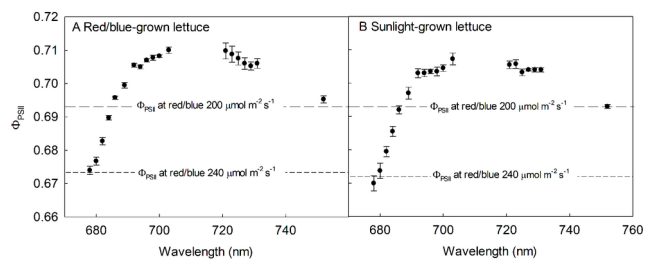


Fig. 4.TIF

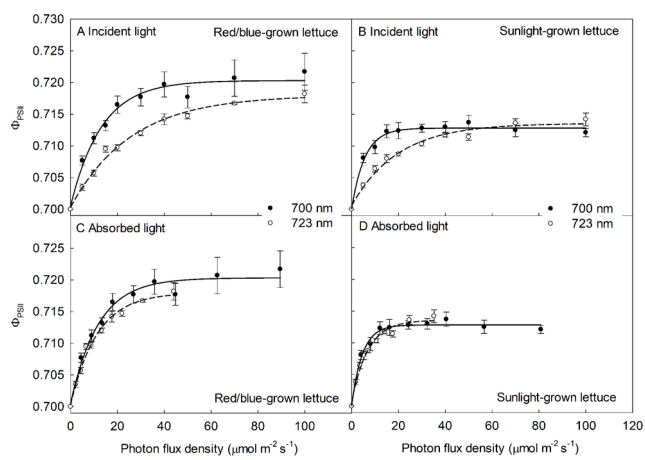


Fig. 5.TIF

Table 1. Morphology (n = 6) and pigment concentration (n = 3) of lettuce grown under red/blue LED light or sunlight. Leaf area represents the total leaf area of three mature leaves from each plant. SLA, specific leaf area. Chl, chlorophyll

Growth light type	Leaf area (cm ²)	SLA (cm ² g ⁻¹)	Carotenoids (mg m ⁻²)	Chl (a+b) (mg m ⁻²)	Chl a/b ratio
Red/blue	280.2	302.8	77.3	528.1	2.74
Sunlight	605.3	352.4	56.0	305.0	2.75
<i>P</i> -value	<0.0001	0.0017	0.0003	<0.0001	0.73